www.dergipark.gov.tr
ISSN:2148-3736
El-Cezerî Fen ve Mühendislik Dergisi
Cilt: 9, No: 1, 2022 (65-85)

El-Cezerî Journal of Science and Engineering
Vol: 9, No: 1, 2022 (65-85)
DOI : 10.31202/ecjse.942644

ECJSE

Research Paper / Makale

Traction Control and Total Driving Force Distribution Strategy for Electric Vehicles with Four in Wheel Motors based on PD-Fuzzy Control

Islam R. H. SHAMIA[1a], Kemal KESKIN[1b]

[1]Electrical and Electronics Engineering Department, Eskisehir Osmangazi University, Eskisehir, TÜRKİYE
[a]ishamia92@gmail.com

Received/Geliş: 25.05.2021 **Accepted/Kabul:** 16.11.2021

Abstract: In this manuscript, a torque distribution control system is proposed for four-wheel motor electric vehicles in order to manage the traction operation of the vehicle when the vehicle is passing on slippery surfaces and to prevent the slip ratio from reaching excessive values. The driving force control is the main controller in the proposed control system and consists of two control loops. PD-Fuzzy logic and PI-control are applied as wheel speed controller in the inner control loop to improve the stability of the vehicle and support the traction operation of the wheels. In order to retain the total requested driving force, force distribution strategies are obtained when the vehicle moves on the road with a low friction coefficient surface. Also, it works as a yaw moment suppressor when the vehicle runs into split slippery surfaces which improves vehicle performance. The proposed vehicle dynamics and torque distribution control system are simulated using Simulink-MATLAB program. The results of the simulation demonstrated the effectiveness of the proposed method.

Keywords: Torque distribution, Driving force control, Electric vehicles, Fuzzy control

Çekiş Kontrolü ve Dört Tekerlek Motorlu Elektrikli Araçlar için PD-Bulanık Kontrollü Toplam Sürüş Kuvveti Dağıtım Stratejisi

Öz: Bu makalede aracın kaygan yüzeylere geçerken aracın çekiş çalışmasını yönetmek ve kayma oranının aşırı değerlere ulaşmasını önlemek amacıyla dört tekerlekli motorlu elektrikli araçlar için bir tork dağıtım kontrol sistemi önerilmiştir. İtici güç kontrolü, önerilen kontrol sistemindeki ana kontrolördür ve iki kontrol döngüsünden oluşur. PD-Bulanık mantık ve PI-kontrol, aracın dengesini artırmak için iç kontrol döngüsünde tekerlek hız kontrolörü olarak uygulanır. Toplam talep edilen itici gücü korumak için, araç yolda düşük sürtünme katsayılı yüzey ile hareket ettiğinde kuvvet dağıtım stratejileri elde edilir. Ayrıca, araç bölünmüş kaygan yüzeylere girdiğinde bir yalpalama momenti bastırıcı olarak çalışır ve bu da aracın performansını artırır. Önerilen araç dinamikleri ve tork dağıtım kontrol sistemi Simulink-MATLAB Programı kullanılarak benzetilmiştir. Simülasyonun sonuçları önerilen yöntemin etkinliğini göstermiştir.

Anahtar Kelimeler: Tork dağılımı, İtici güç kontrolü, Elektrikli araçlar, Bulanık kontrol

1. Introduction

The manufacturing of electric vehicles (EVs) has gotten a lot of attention in recent years, considering it more efficient in eliminating environmental noise and pollution comparing with internal combustion electric vehicles (ICEVs) [1-3]. The interest in EVs has steadily increased in the last 20 years due to the reduction in fossil fuel resources and growth of environmental emissions. EVs are considered a great solution to the issue of reliance on petrol and the global energy resources problem [4, 5]. Moreover, utilizing electric motors and inverters in EVs provides

How to cite this article
Shamia, I., Keskin, K., "*Traction Control and Total Driving Force Distribution Strategy for Four-Wheel-drive Electric Vehicles based on PD-Fuzzy Control*" El-Cezerî Journal of Science and Engineering, 2021, 8(2); 65-85.

Bu makaleye atıf yapmak için
Shamia, I., Keskin, K., "Çekiş Kontrolü ve Dört Tekerlek Motorlu Elektrikli Araçlar için PD-Bulanık Kontrollü Toplam Sürüş Kuvveti Dağıtım Stratejisi" El-Cezerî Fen ve Mühendislik Dergisi 2021, 8(2); 65-85.
ORCID ID: [a]0000-0002-3275-7898; [b]0000-0002-3969-2396

advantages over ICEVs, just like faster torque response, ease of applying torque allocation optimization, and accuracy of output torque measurement by measuring motor current [6-8]. EVs equipped with four in-wheel independent motors propose many advantages such as the capability of controlling the traction or braking torque of each wheel independently, increasing safety efficiency, and improving overall vehicle dynamic performance [9, 10]. EVs can also control the action of the four wheels through the use of in-rotor motors, without the need for mechanical connections, which is increasing the total operational efficiency and enhancing the control flexibility and accuracy [11].

According to previously mentioned advantages, many research proposed several traction methods to prevent slipping on roads with a low friction coefficient. For instance, [12] proposed a torque blended control system as a traction method for EVs based on sliding mode control and using torque observer, then to enhance referencing of traction torque for each wheel they developed a computational-intelligence device. In [13] by predicting the maximum active forces on four in-wheel EVs presented a developed anti-slip control system as a traction control on different road types tests. In [14, 15] slip ratio control system is proposed based on the dynamical fuzzy control system using sliding mode and estimated slip ratio for longitudinal vehicle motion. On the other hand, many studies proposed driving torque distribution from an economical perspective, which means they consider power saving distribution control strategies based on traction control system, motor model, and total feedback energy from the system [5, 16-19].

For EVs with four in-wheel motors, a torque distribution strategy and traction control system are proposed in this paper. By considering the driving force controller as the main control in the proposed method, the traction control method was originally developed to control the total driving force and longitudinal slip based on PD-Fuzzy logic controller and PI controller, in order to achieve the requested driving force by a user without significant effects on the vehicle performance. The driving force distribution method is applied depending on the pre-defined experimental roads, which enhance the vehicle stability by preventing the slip ratio from reaching the upper or lower limits, also suppressing the generated yaw moment between the right and left side's wheels.

In the case when the vehicle enters into a split slippery surface sheet the forces will distribute depends on the situation of each wheel to suppress the generated yaw-moment and retain the total driving force. In addition, when the vehicle runs into the full slippery surface sheet, the force distribution between the front and rear wheels depends on which wheels still have traction on the normal surface with high slippage.

2. Methods and Models

In order to enhance the total performance of Electric vehicles, studies on vehicle dynamics had huge attention from the developers in the automotive industry. In this section, proposed vehicle dynamics and experimental vehicle properties are explained.

2.1. Experimental Vehicle Properties

The authors of [7] developed the experimental *(KANON-FPEV2),* with four in-wheel motors and outer-rotor-type in many applications in their studies. The properties and parameters of the experimental vehicle are presented~~,~~ in Table 1.

2.2 Vehicle Dynamics and Modeling:

As the major goal in this research is driving force distribution control, the illustrated vehicle dynamics equations and modeling are taken into account only the longitudinal motion of the vehicle and rotational motion of the four wheels, as presented in Figures 1 and 2.

The equations of longitudinal motion for vehicle body and rotational motion for each wheel of the proposed vehicle model are described as the following equations:

$$J_n \dot{\omega}_n = T_n - rF_{dn} \quad , \quad n = 1,2,3,4 \tag{2.1}$$

$$M\dot{V} = F_{d1} + F_{d2} + F_{d3} + F_{d4} \tag{2.2}$$

The rotational motion dynamics for each wheel are described in the first equation. Where J (Nm^2) is the inertia of the wheel, ω (rad/s) angular velocity of the wheel, $\dot{\omega}$ (rad/s^2) is the wheel angular acceleration, r (m) represents the actual radius of the wheel, and F_d (N) represents the driving force at the contact area between tire and road. Such T (Nm) is the torque of the motor, and it represents the delivered torque to the wheel by assuming the requested torque applied directly on each wheel.

Table 1. Properties and parameters of the *KANON-FPEV2* model [7].

#	Name	Unit	QTY
1	Max. Torque of the Front in-wheel motor	Nm	500 ±
2	Max. Torque of the Rear in-wheel motor	Nm	340 ±
3	Mass of the Vehicle	Kg	870
4	The base of the Wheel	meter	1.7
5	Distance between gravity center and front axel	meter	0.99
6	Distance between gravity center and rear axel	meter	0.701
7	Base of Tread	meter	1.3
8	The Wheel Radius	meter	0.302

In the second equation, the dynamics of the vehicle while running on a straight path with the same steering angles for each wheel are presented. Such M (Kg) is the total mass of the vehicle, $\dot{V}$ (m/s^2) represents the acceleration of the vehicle, and V (m/s) is the velocity of the vehicle. Furthermore, n = 1, 2, 3, 4 are indices for (front right wheel, front left wheel, rear right wheel, rear left wheel) respectively.

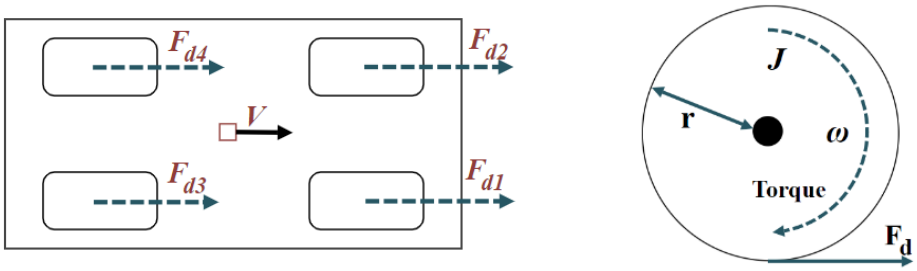

Figure 1. Dynamics of the longitudinal and rotational motion for each wheel.

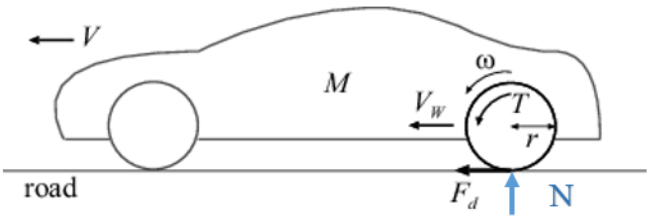

Figure 2. Applied normal force and Dynamics of the longitudinal motion.

The type of road surface and road friction coefficient are major factors in the driving force F_d calculation, and it can be defined as the follows:-

$$F_{dn} = \mu(\lambda_n)_n N \tag{2.3}$$

$$N = \frac{M}{4} \times g \tag{2.4}$$

where $\mu(\lambda)$ represent the friction coefficient for each wheel and its calculated as a function of the slip ratio (λ), N represent the applied normal force on the tire where it is supposed to be equal for all vehicle wheels and, and g represents the force of gravity.

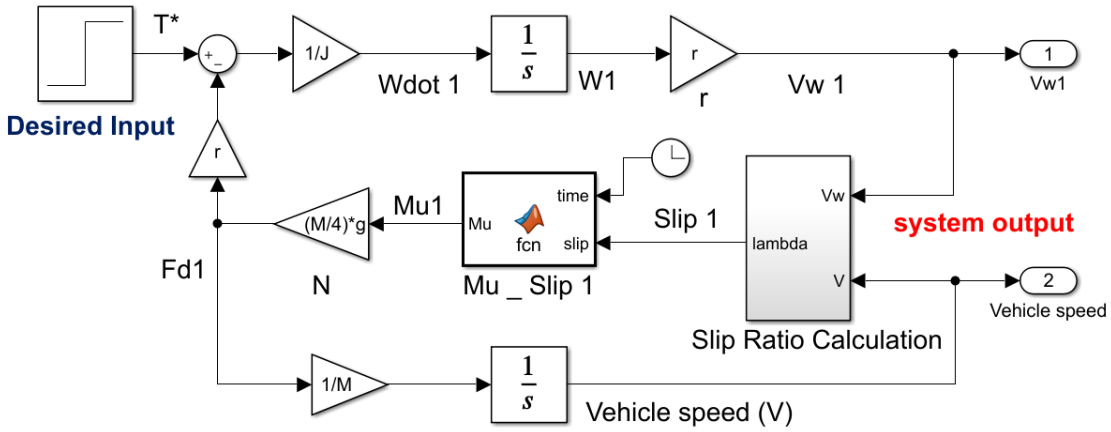

Figure 3. Single wheel vehicle block diagram

1.1. Tire Model

The applied normal force on the vehicle wheels while moving in a straight way generates friction in the contact area between tire and road due to deformation and interaction between tire and type of road [20, 21]. The resultant friction forces have three types of mechanisms, adhesion friction, deformation friction, and wear friction. This occurs due to sticking and deforming rubber to complete the tiny irregularities when the tire moves on the road surface [22, 23].In this paper, the main function that describes friction coefficient and its relation with longitudinal slip ratio is written based on Pacejka's Magic formula[24, 25], which is described as the following equation:-

$$\mu(\lambda_n)_n = D \times \sin\left\{C \times \arctan\left[B \times \lambda_n - E \times (B \times \lambda_n - \arctan(B \times \lambda_n)\right]\right\} \tag{2.5}$$

B is the stiffness coefficient, C is the shape coefficient, D is the peak coefficient, and E is the curvature factor. Where λ_n is the slip ratio for each wheel, values of road condition factors are explained, as described in Table 2.

Table 2. Values of Magic Formula parameters for main different road conditions [24, 25].

Types of roads	Dry road	Wet road	Snow surface	Icy surface
B	10	12	5	4
C	1.9	2.3	2	2
D	1	0.82	0.3	0.1
E	0.97	1	1	1

1.2. Slip Ratio Calculation

The longitudinal slip ratio is the ratio of the difference in vehicle speed and wheel speed caused by rubber deformation in the contact region between tire and road surface while the vehicle is driving in a straight path [21, 26]. The equations of longitudinal slip ratio for driving and braking situation are explained as the following equations:

$$\lambda_n\left(\omega_n, V_n\right)=\frac{V\,\omega_n - V_n}{\max\left(V\,\omega_n, V_n, \varepsilon\right)} \quad , \textit{ for driving} \tag{2.6}$$

$$\lambda_n\left(\omega_n, V_n\right)=\frac{V_n - V\,\omega_n}{\max\left(V\,\omega_n, V_n, \varepsilon\right)} \quad , \textit{ for braking} \tag{2.7}$$

$$V\,\omega_n = \omega_n \times r \tag{2.8}$$

where V is the vehicle velocity, ε is a small positive number to prevent division by zero. Also, $V\omega$ is the wheel velocity, which is described as the product of wheel angular velocity and wheel radius. The proposed slip ratio block diagram for driving mode is explained, as shown in Figure 4.

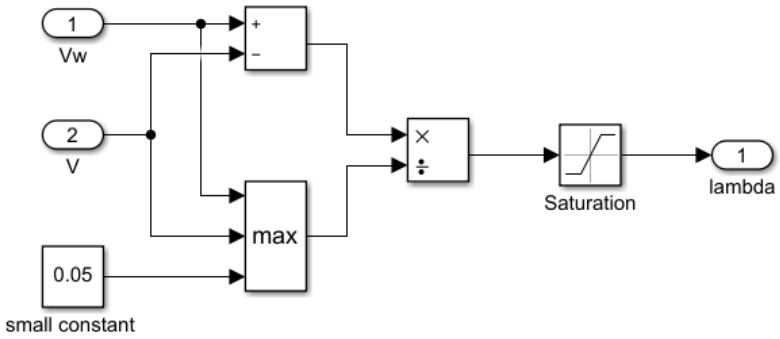

Figure 4. Longitudinal Slip ratio calculation for each wheel block diagram.

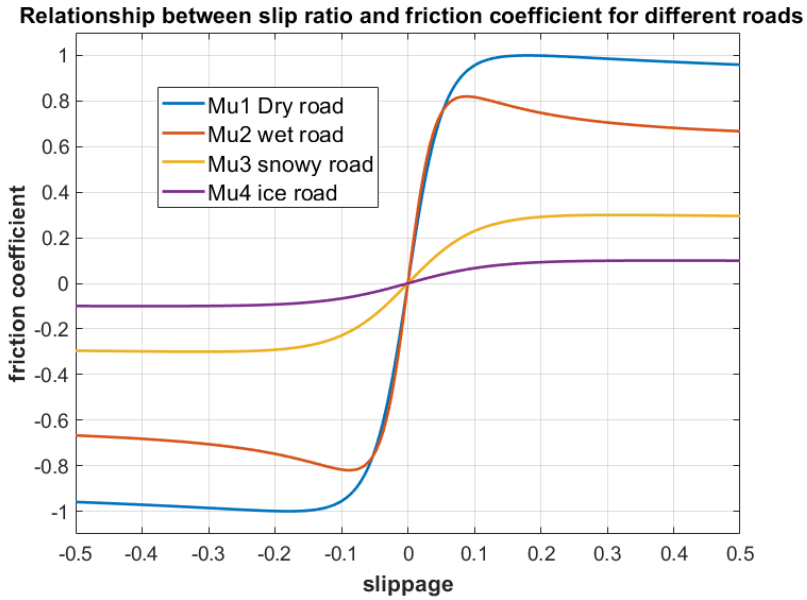

Figure 5. The relationship between longitudinal Slip and Friction Coefficient.

There are two peaks for each curve in the $\mu - \lambda$ relation and it depends on the types of roads. The μ value is rising proportionally as a function λ while λ is rising and still inside the domain of maximum and minimum peaks. As well as the μ value is decreasing as a function of λ while the

absolute of λ values increase in the outside of max and min [24, 25]. The $\mu - \lambda$ relation for different road conditions based on the Magic formula from equation (3.5) is presented, as shown in Figure 5.

The maximum positive peak values of the previously mentioned friction coefficient for main common road surfaces are explained, as shown in Table 3.

Table 3. The maximum friction coefficient for different road surfaces

Type of road surface	μ_1 Dry road	μ_2 Wet road	μ_3 Snow road	μ_4 Icy road
Maximum friction coefficient	0.9 – 1	0.8 – 0.85	0.2	0.1

2. Driving Force Control and Distribution Method

In this section, the proposed driving force control system and distribution strategies for EV with four in-wheel motors while moving on instantaneous split and slippery surface sheets are presented. Controllers like wheel speed and driving force controllers are implemented with different control methods. The performance of each system is compared in order to increase the reliability and effectiveness of the applied approaches which enhance the vehicle performance.

2.1. Driving Force Controller and $\lambda - Y$ relation

The configuration of the obtained driving force controller has two control loops, and the first is an outer control loop that manages the driving force using feedback from the driving force observer. The second loop is an inner control loop that regulates the speed of each wheel in order to keep the vehicle's slip ratio under control, as presented in Figure 6.

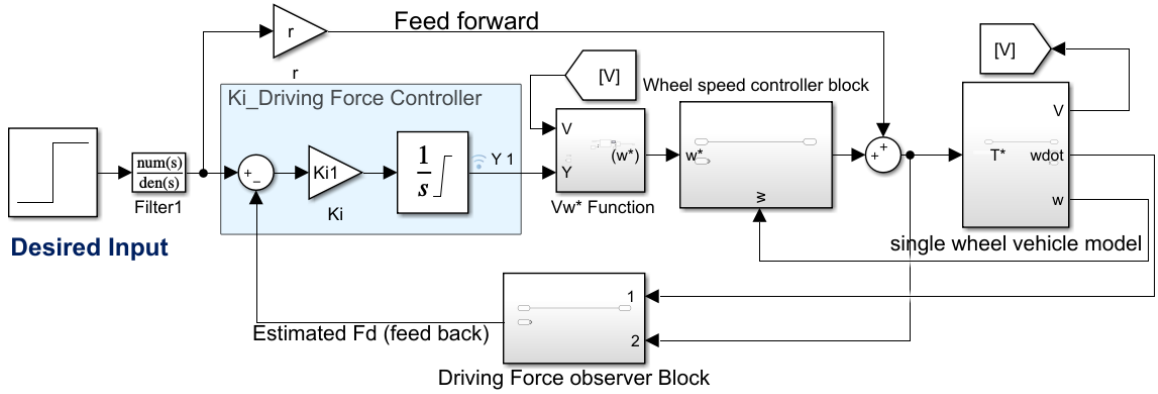

Figure 6. The Proposed driving force control system.

Depending on the defined driving force equation (2.3), the relation between the $\boldsymbol{\lambda}$ of each wheel and the F_d can be described as the driving stiffness. The driving stiffness for each wheel can be calculated as the following equation:

$$Ds_n = \frac{F_{dn}}{\lambda_n} \tag{3.1}$$

where Ds is the driving stiffness for each wheel, F_d is the driving force, and λ represents the longitudinal slip ratio.

In the case of acceleration, the wheel speed is greater than the vehicle's speed ($V\omega \geq V$) and the slip ratio calculated as written in equation (2.6). Conversely, in the case of deceleration, the wheel speed becomes less than the speed of the vehicle ($V\omega < V$), and the slip ratio is found by different formula as described in equation (2.7). Accordingly, the definition of slip ratio must be alternated while applying different control commands, which makes λ not convenient to apply it directly in the plant of the driving force controller. Consequently, the definition of controller Y is developed as a function of vehicle and wheel speed for all driving modes for utilizing it as controller input instead ofλ, as described in equation 3.2.

$$Y_n = \frac{V\,\omega_n}{V_n} - 1 \tag{3.2}$$

The relationship between Y and λ for both driving or braking situation is defined as the following equation:

$$Y_n = \begin{cases} \dfrac{\lambda}{1-\lambda} & , \ for\ driving \\ \lambda & , \ for\ braking \end{cases} \tag{3.3}$$

Figure 7. Presents the curve of (Y – slip ratio) relationship, and it shows that while the magnitude of slip ratio value is much less than 1 ($|\lambda| \ll 1$) then slip ratio equals to Y. According to that, it is appropriate to apply Y in the controller instead of λ and equation (3.1) can be written like $F_d = D_s \times \lambda$, while considering ($|\lambda| << 1$).

By assuming the transfer function from Y to F_d be zero-order and depending on the ($Y-\lambda$) relation, the driving force controller's transfer function can be described as:

$$F_d = D_s \times Y \cong D_s \times \lambda \quad , such \quad Y \cong \lambda \tag{3.4}$$

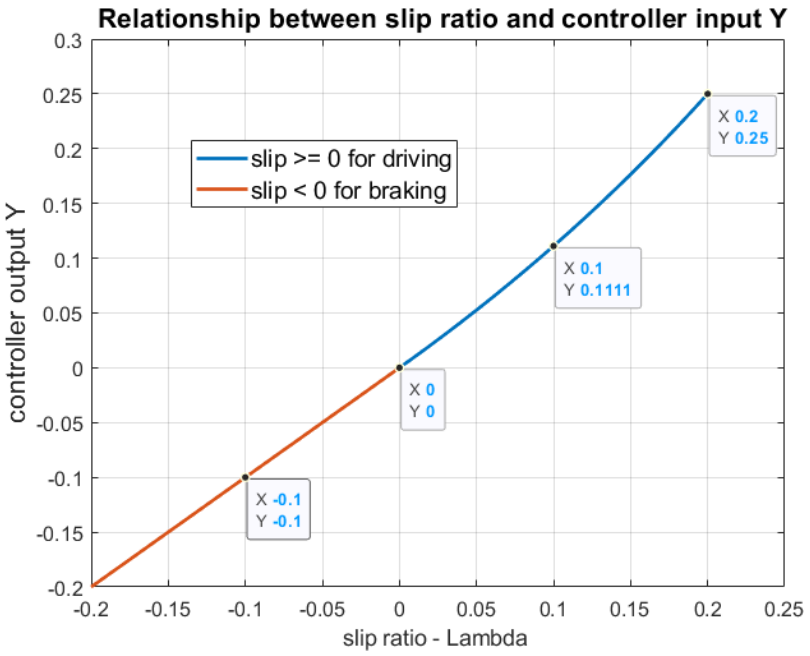

Figure 7. The curve of (Y – *slip ratio*) relationship.

The proposed driving force controller has one controller, which is a limited gained integrator, the input of the control system is desired driving force F_d and it is defined by the user (driver), the output of the controller is Y as the difference between desired F_d and feedback F_d coming from driving force observer, as shown in Figure 8.

The upper and lower boundaries of the integrator are obtained on the Y output based on the maximum and minimum peaks from $(\lambda - \mu)$ relation and the relation between $(\lambda - Y)$. The initial value of Y_0 is defined as equal to zero, and the upper and lower boundaries for both Y and λ are described as shown in Table 4. The aims of applying these boundaries are to keep the slip ratio (λ) inside the range where friction coefficient is monotonic with λ, also to keep Y and slip ratio (λ) values within the range where $(Y \cong \lambda)$ satisfied.

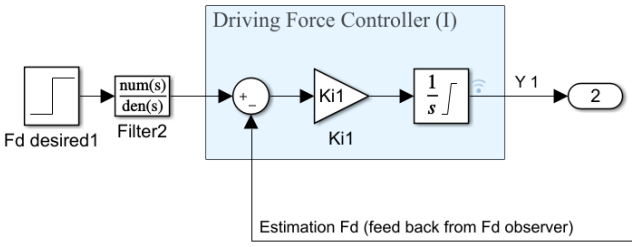

Figure 8. Driving force controller block diagram.

Table 4. Maximum and minimum values for Y and λ.

Name	Value
Y_{max}	0.25
Y_{min}	- 0.20
λ_{max}	0.20
λ_{min}	- 0.20

2.2. Desired Wheel Speed ($V\omega$*) and Angular Velocity (ω*) Calculations

The inputs of the inner control loop (wheel speed controller) are defined based on the output of driving force controller Y and vehicle body velocity V. From equation (3.2), the desired wheel speed ($V\omega$*) and angular velocity (ω*) as a reference for the wheel speed controller can be defined as the following equation:

$$V\,\omega^* = V + Y \times V \tag{3.5}$$

$$\omega^* = \frac{V\,\omega^*}{r} \tag{3.6}$$

According to equation (3.5), since the initial V_0 of a vehicle is defined to be zero $(V_0 = 0)$, desired calculated wheel speed ($V\omega$*) in the starting operating will remain equal to zero regardless of the Y value. To avoid this problem, the desired wheel speed ($V\omega$*) calculating formula is redefined by adding a small constant (σ) instead of vehicle speed value in the case that the vehicle speed (V) is less than (σ), as described in the following equation:

$$V\,\omega^* = \begin{cases} V + (Y \times \sigma) \;, & (V < \sigma) \\ V + (Y \times V) \;, & (V \geq \sigma) \end{cases} \tag{3.7}$$

2.3. Driving Force Observer:

The main purpose of the proposed driving torque observer is to calculate the estimated driving force for each wheel in the vehicle as a feedback for the outer loop of the driving force control system. Depending on the equation (2.1), and vehicle dynamics, the presented driving force observer ~~is~~ consist of two main input and one output, as shown in Figure 9.

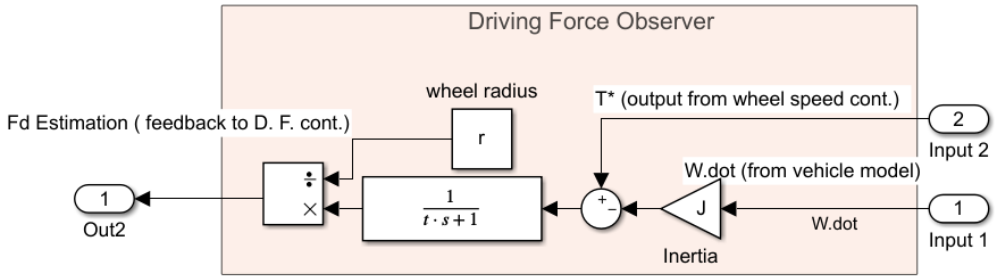

Figure 9. Driving Force Observer block diagram.

2.4. Wheel Speed Controller:

In the proposed driving force control system, the wheel speed controller represents the inner loop controller, and it is explained in this section. The main objectives of applying wheel speed controller are explained as follows:

- Reach to the desired wheel speed as well as Prevents slip and support the vehicle traction when the vehicle runs into a split or slippery surface sheet.
- Control on the delivered torque for each wheel.

The input of this controller is the desired wheel angular velocity W* and The Feedback comes from the calculated actual wheel angular velocity in the vehicle model. The output of the controller is the desired delivered torque T*. Moreover, in the interest of increasing the system response, driving torque ($r*F_d$) is added to the output of the system as a feed-forward, as shown in Figure 10.

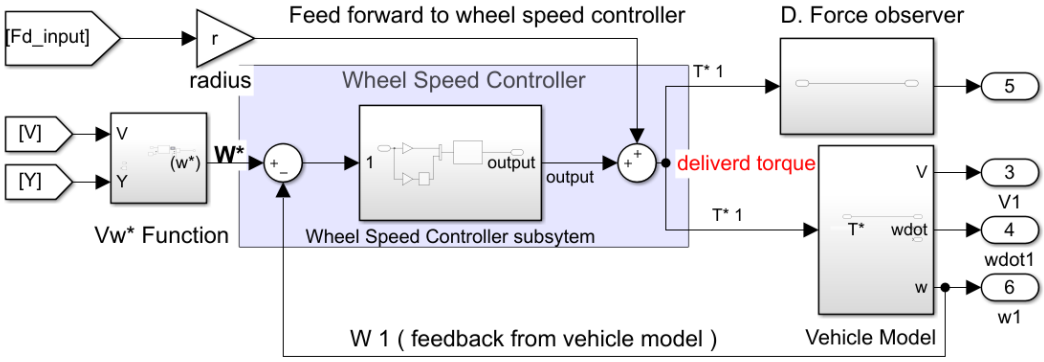

Figure 10. Wheel speed controller main Block diagram

Two types of control systems are applied and compared in the same simulation situation in order to contribute to this research.

Wheel Speed Controller Based on Fuzzy Logic Control with PD (Proportional-Derivative gains) parameters:

In this section, Fuzzy logic with PD-gains control system as a wheel speed controller is presented, as shown in Figure 11.

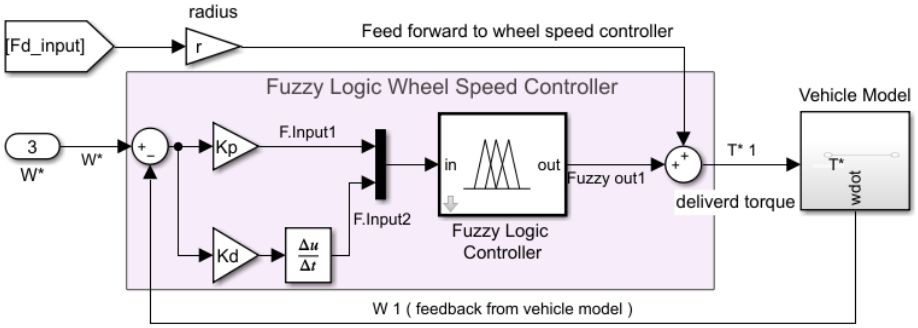

Figure 11. Wheel speed controller based Fuzzy Logic controller Block Diagram.

During the experimental trials, P, I and D gains were tried to be selected in the most appropriate way. The gains were tried by aiming to decrease the maximum overshoot, rise time and settling time and it was concluded that the integral gain did not contribute towards the purpose. Therefore PD controller was chosen as a part of Fuzzy logic control. The proposed PD-Fuzzy logic control system consists of two fuzzy inputs and one output. The first input is the error value between the desired wheel angular velocity and the actual generated output angular velocity from the vehicle model and it is connected with proportional gain. The second input is the change in the error and it is connected with derivative gain. The output of the controller is the delivered torque for each wheel *(T*).*

The Fuzzy logic controller consists of three main stages, Fuzzification, Inference (Fuzzy rules), and Defuzzification, as shown in Figure 12. The Mamdani method is used to design the fuzzy controller, and the centroid method is used in the defuzzification stage.

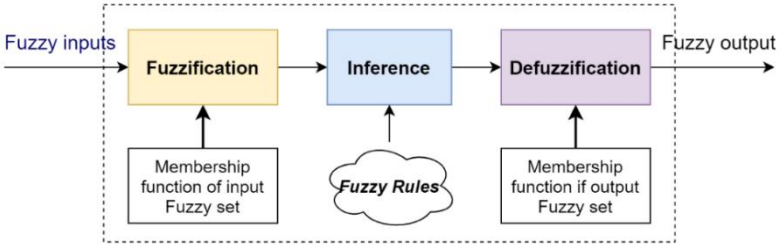

Figure 12. Fuzzy Logic controller Block diagram.

Fuzzy membership function and Fuzzy Rules

The fuzzy input 1 and fuzzy input 2 are defined as the error and the change in the error (Table 5). The membership functions of both of two inputs are defined as [N2, N1, ZE, P1, P2] with range [-1 1]. The type of applied membership functions and parameters for each input are described, as shown in Figures 13 and 14.

Table 5. Fuzzy inputs and outputs

Fuzzy Inputs	Error (the difference between desired speed and actual speed) Change of Error (derivative of error)
Fuzzy Output	Proportional constant (to adjust the delivered torque)

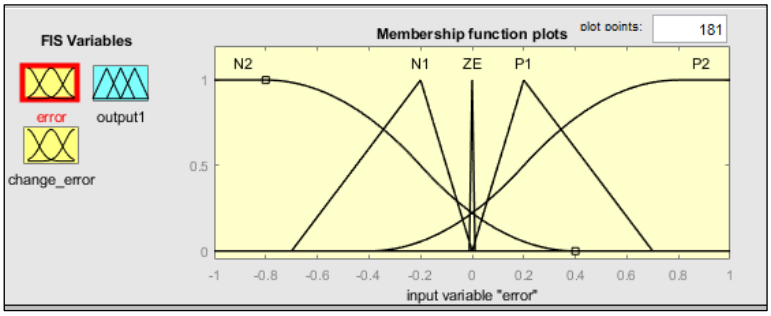

Figure 13. Membership functions of Fuzzy logic input 1. (Error).

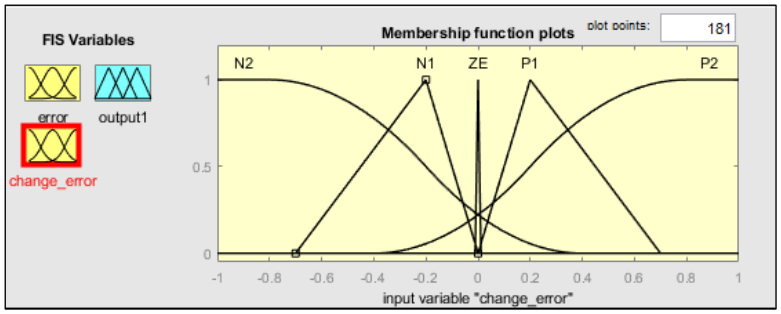

Figure 14. Membership functions of Fuzzy logic input 2. (Change of Error).

The fuzzy output is the output of the wheel speed controller (Table 5). The membership functions of the Fuzzy output are divided into five membership [N2, N1, ZE, P1, P2]. The range of each membership function is [-10 10]. The type of applied membership functions and parameters of each MF in the fuzzy output is explained, as shown in Figure 15.

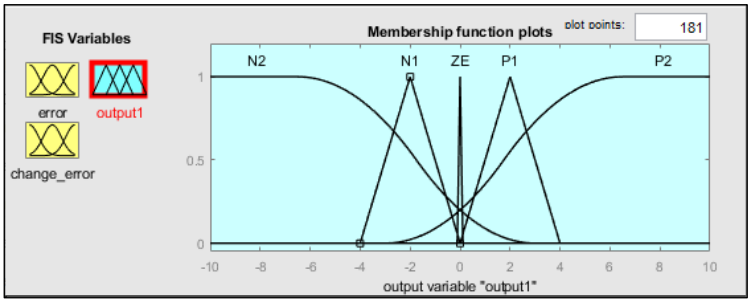

Figure 15. Membership functions of Fuzzy logic output.

The implemented Fuzzy rules, where N2 represents negative big, N1 represents negative small, ZE represents zero, P1 is positive small, and P2 represents positive big are described, as shown in Table 6.

Table 6. Rules of Applied Fuzzy Logic controller.

		Input 2 (Change in Error)				
		N2	**N1**	**ZE**	**P1**	**P2**
Input 1 (Error)	**N2**	N2	N2	N1	N1	ZE
	N1	N2	N1	N1	ZE	N1
	ZE	N1	N1	ZE	P1	P1
	P1	N1	ZE	P1	P1	P2
	P2	ZE	N1	P1	P2	P2

Wheel Speed Controller Based on PI control (Proportional-Integral gains) parameters:

In this section, the PI (Proportional-Integral gains) control system as a wheel speed controller is presented, as shown in Figure 16.

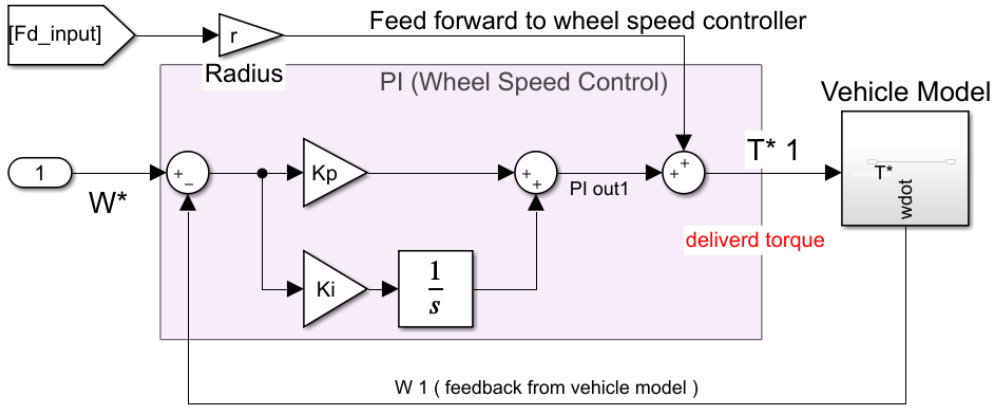

Figure 16. PI controller Block diagram.

3. Proposed Driving Force Distribution Method:

Force distribution coefficient phi (∅) is defined to write the distribution equations. In the case when the vehicle runs into a road with high friction coefficient, the total requested driving force is distributed evenly on the four wheels, the main force distribution equation is presented as the following equation:

$$Fd_n = Fd_{\text{total}} \times \phi_{\text{main}} \tag{3.8}$$

where $\emptyset_{main}$ is the main distribution coefficient, and it is always equal to %25.

In the case when the vehicle runs into a split slippery surface sheet on the right side, the distribution is applied on the front and right side's wheel to reduce the total slip ratio value of the vehicle. Also smaller distribution is applied on the left side's wheels at the same time to enhance the traction operation. Moreover, when the vehicle runs into a full slippery road, the total driving force is distributed between the front and rear wheels.

Based on short split/slippery surface sheets, two intervals for slippery sheets are defined on the Front and Rear wheels during the simulation. In the first interval, only the front wheels move on the slippery sheet, and in the second interval, only the Rear wheels move on the slippery sheet.

- **Distribution equations in the interval (a) :**

$$Fd_1 = Fd_{total} \times \phi_{main} \times \phi_{1a} \tag{3.9}$$
$$Fd_2 = Fd_{total} \times \phi_{main} \times \phi_{2a} \tag{3.10}$$
$$Fd_3 = Fd_{total} \times \phi_{main} \times \phi_{3a} \tag{3.11}$$
$$Fd_4 = Fd_{total} \times \phi_{main} \times \phi_{4a} \tag{3.12}$$

- **Distribution equations in the interval (b) :**

$$Fd_1 = Fd_{total} \times \phi_{main} \times \phi_{1b} \tag{3.13}$$
$$Fd_2 = Fd_{total} \times \phi_{main} \times \phi_{2b} \tag{3.14}$$
$$Fd_3 = Fd_{total} \times \phi_{main} \times \phi_{3b} \tag{3.15}$$
$$Fd_4 = Fd_{total} \times \phi_{main} \times \phi_{4b} \tag{3.16}$$

4. Simulation Results and Discussion:

Simulink-MATLAB is the simulation platform of the vehicle dynamics and proposed Torque distribution control system. The parameters of the proposed control system are presented, as shown in Table 7.

Table 7. Simulation Parameters of the proposed Controller.

Name	Description	Value
Ki1	I gain _ driving force controller for both of PI and Fuzzy module	0.001
Kp_{fuzzy}	P gain _ wheel speed controller _ Fuzzy	55
Kd_{fuzzy}	D gain _ wheel speed controller _ Fuzzy	0.01
Kp_{PI}	P gain _ wheel speed controller _ PI	1230
Ki_{PI}	I gain _ wheel speed controller _ PI	1925
Fd_{Total}	Total requested desired driving force	1000
V_0	Initial velocity	0
ε	Small Positive number	0.05
σ	Small positive number	0.1
μ	Friction Coefficient of the slippery sheet	0.15

Simulation is applied in two types of experimental roads by using two different types of controllers, PD-Fuzzy logic controller and PI controller. In the first experimental road, a split slippery sheet is implemented on the right side of the vehicle, and the length of the sheet is supposed to be equal to 1 second. The first slip interval will start after 6 seconds from start driving with a length of 1 second on the front right wheel and the second slip interval after 8 seconds with a length of 1 second on the rear wheel, as shown in Figure 17.

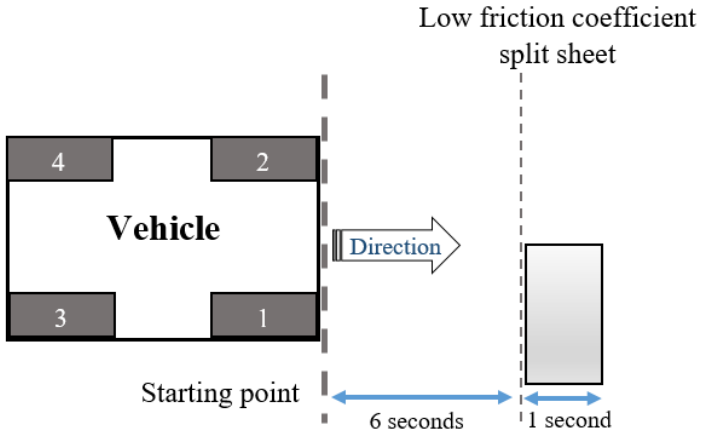

Figure 17. First experimental road description using Split Slippery Sheet.

For the first experimental road, the distribution coefficient for each wheel is described, as shown in Table 8. In the second experimental road, a full slippery sheet is implemented on both of right and left sides of the vehicle, and the length of the sheet is supposed to be equal to 1 second. The first slip interval will start after 6 seconds from start driving with a length of 1 second on the front wheels, and the second slip interval after 8 seconds with a length of 1 second on the rear wheels, as shown in Figure 18.

Table 8. Distribution coefficient for each wheel _ Split slippery sheet.

Name	Description	Value
$\emptyset_{main}$	Main distribution coefficient	0.25
$\emptyset_{1a}$	First slip interval _ Front Right wheel _ distribution coefficient	0.5
$\emptyset_{2a}$	First slip interval _ Front Left wheel _ distribution coefficient	0.75
$\emptyset_{3a}$	First slip interval _ Rear Right wheel _ distribution coefficient	1.5
$\emptyset_{4a}$	First slip interval _ Rear Left wheel _ distribution coefficient	1.25
$\emptyset_{1b}$	Second slip interval _ Front Right wheel _ distribution coefficient	1.5
$\emptyset_{2b}$	Second slip interval _ Front Left wheel _ distribution coefficient	1.25
$\emptyset_{3b}$	Second slip interval _ Rear Right wheel _ distribution coefficient	0.5
$\emptyset_{4b}$	Second slip interval _ Rear Left wheel _ distribution coefficient	0.75

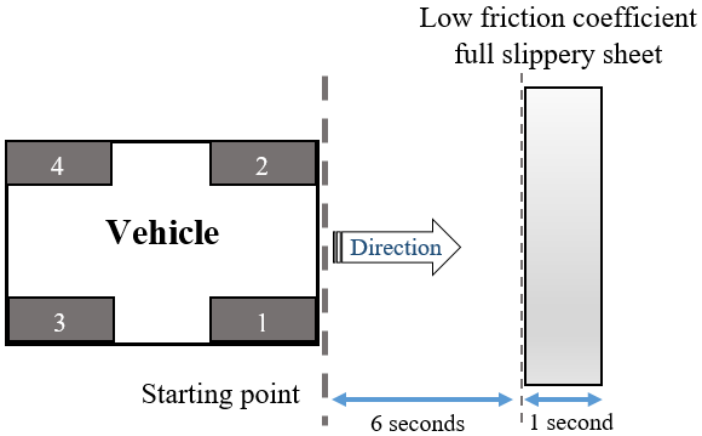

Figure 18. Second experimental road description using Full Slippery Sheet.

For the second experimental road, the distribution coefficient for each wheel is described, as shown in Table 9.

Table 9. Distribution coefficient for each wheel _ Full slippery sheet.

Name	Description	Value
$\emptyset_{main}$	Main distribution coefficient	0.25
$\emptyset_{1a}$	First slip interval _ Front Right wheel _ distribution coefficient	0.5
$\emptyset_{2a}$	First slip interval _ Front Left wheel _ distribution coefficient	0.5
$\emptyset_{3a}$	First slip interval _ Rear Right wheel _ distribution coefficient	1.5
$\emptyset_{4a}$	First slip interval _ Rear Left wheel _ distribution coefficient	1.5
$\emptyset_{1b}$	Second slip interval _ Front Right wheel _ distribution coefficient	1.5
$\emptyset_{2b}$	Second slip interval _ Front Left wheel _ distribution coefficient	1.5
$\emptyset_{3b}$	Second slip interval _ Rear Right wheel _ distribution coefficient	0.5
$\emptyset_{4b}$	Second slip interval _ Rear Left wheel _ distribution coefficient	0.5

The simulations are compared with three different situations for each proposed control system and distribution strategy for each experimental road.

- Simulation without applying any type of traction control or distribution methods.

- Simulation using proposed control system without applying distribution strategies.
- Simulation using proposed control system and distribution strategies.
- Comparison between proposed PD-Fuzzy Logic controller and PI controller.

The simulation results for each previously mentioned situation and different experimental road conditions are explained as follows:

The results of applying 250 N driving force on each wheel without implementing any control on the system are presented, as shown in Figure 19.

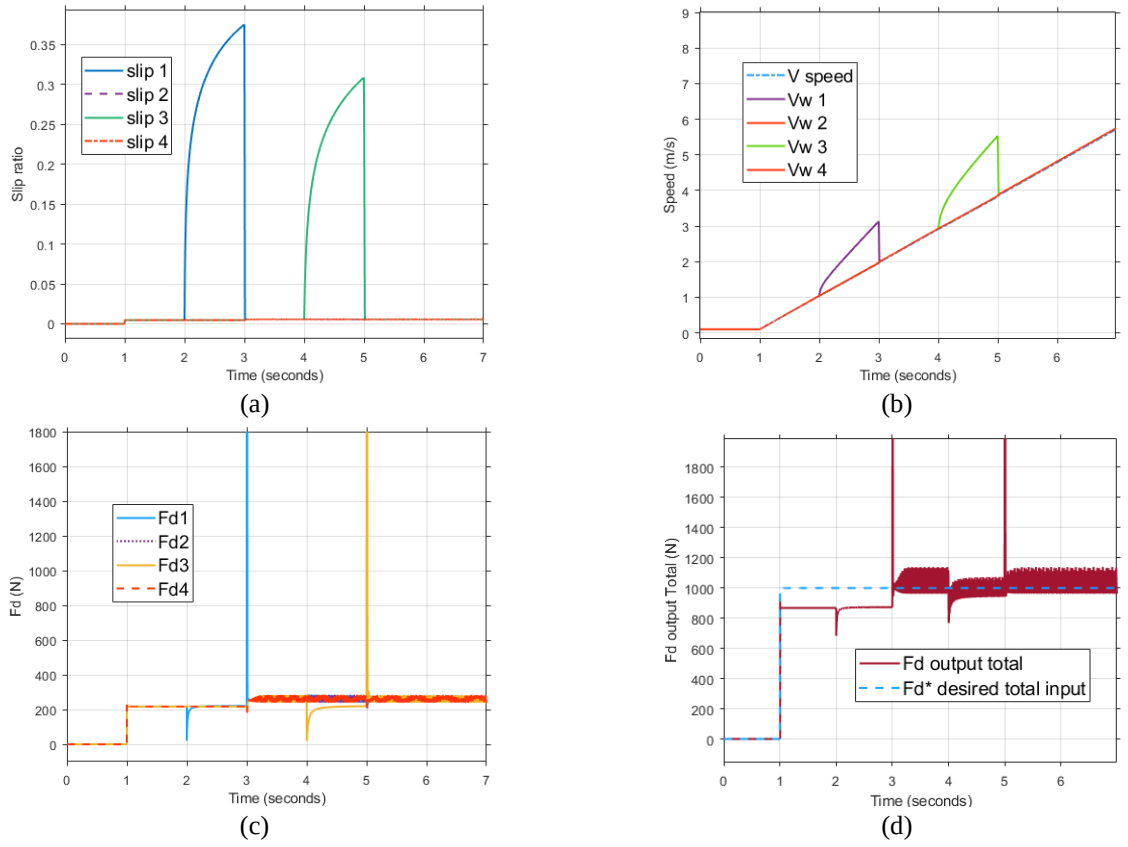

Figure 19. Simulation results of split slippery sheet (without control or distribution). (a) Slip ratio, (b) vehicle & wheel speed (c) driving force F_d (d) total output driving force $F_{d\ total}$

In Figure 19, an extreme slip occurs on the right wheels of the vehicle, which saturates the driving force of the right side's wheels. In addition, an extreme disturbance occurred, and the total output driving force is much less than the optimal value.

In the case when applying control system without a distribution strategy, the total driving force is distrusted equally to be 250 [N] for each wheel.

Figures 20 presents the results of applying total driving force = 1000 N, while vehicle runs into first experimental road (split slippery sheet) using only the proposed driving force control methods without apply distribution strategy.

The slip ratio results are better comparing with results without applying controller on the systems but it's still high and reached the upper limits for slip then saturated when vehicles run on the

slippery sheet. Because of that, driving force and delivered torque for the right side wheels are decreased between 6-7th second for the front right wheel, and between 8-9th for the rear right wheel, which is made a big disturbance on the vehicle driving force. Consequently, the total output driving force could not be retained, and exceeded the maximum limits of in-wheel motor torques. A huge Yaw-moment generated between the total left and right sides applied driving force, which directly affects the vehicle stability and reduces the safety of driving.

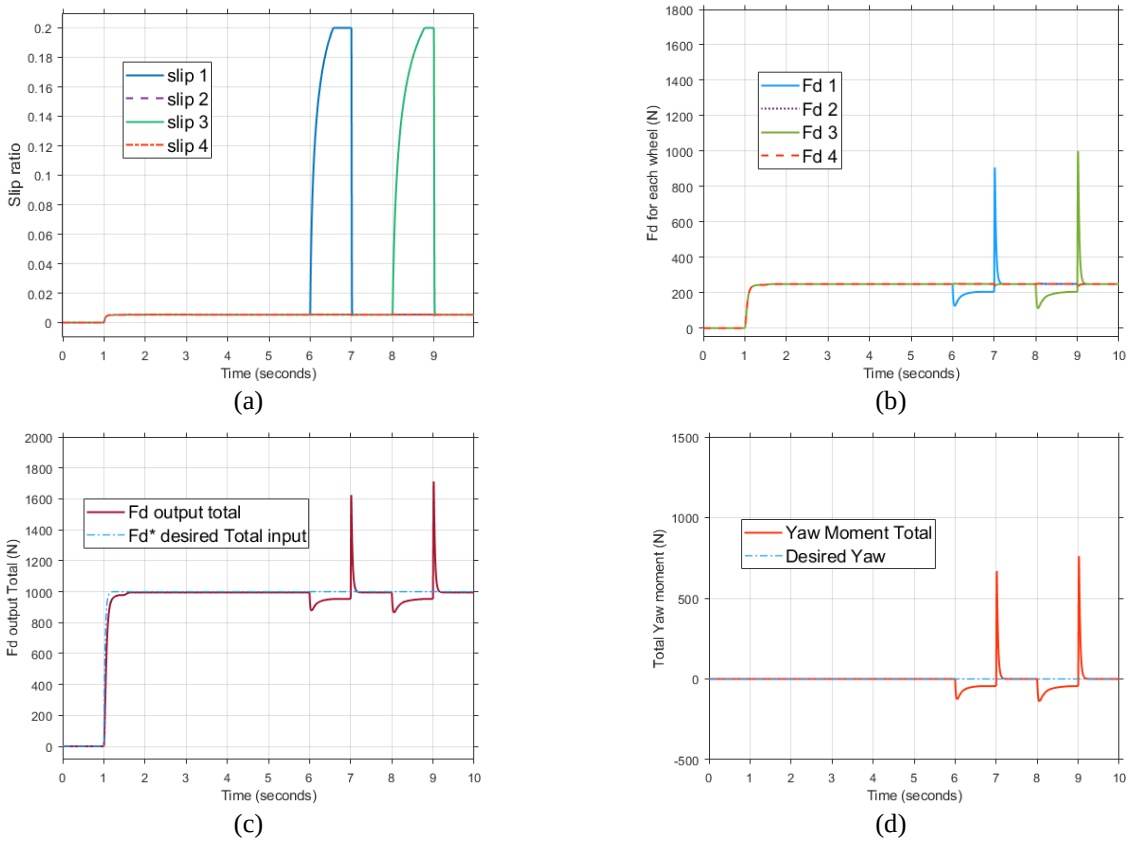

Figure 20. Simulation results of split slippery sheet (only PD-Fuzzy control). (a) Slip ratio, (b) driving force F_d (c) total output driving force $F_{d\,total}$ (d) Yaw-moment output.

Figures 21 presents the simulation results of the proposed control system with the proposed distribution method when vehicle move on the first experimental road. The Total input driving force distributed between the four wheels based on the situation of each wheel. Consequently, the delivered torques for each wheel are distributed too.

As a result, the slip ratio results while applying distribution strategies when the vehicle moves on a split slippery sheet are too small and didn't exceed (0.025) for the right side's wheels. Which is a negligible slip for both of PD-Fuzzy and PI controller. The same results proofed by comparing the vehicle speed and wheels speed for both of the two controllers. The total driving force for both of PD-Fuzzy and PI are retained without effects on the traction operation, also the generated yaw-moment is suppressed successfully, which can be confirmed by comparing figures (20) with (21).

Figures 22 the results of applying total driving force = 1000 N, while vehicle runs into second experimental road (full slippery sheet) using only the proposed driving force control methods without apply distribution strategy.

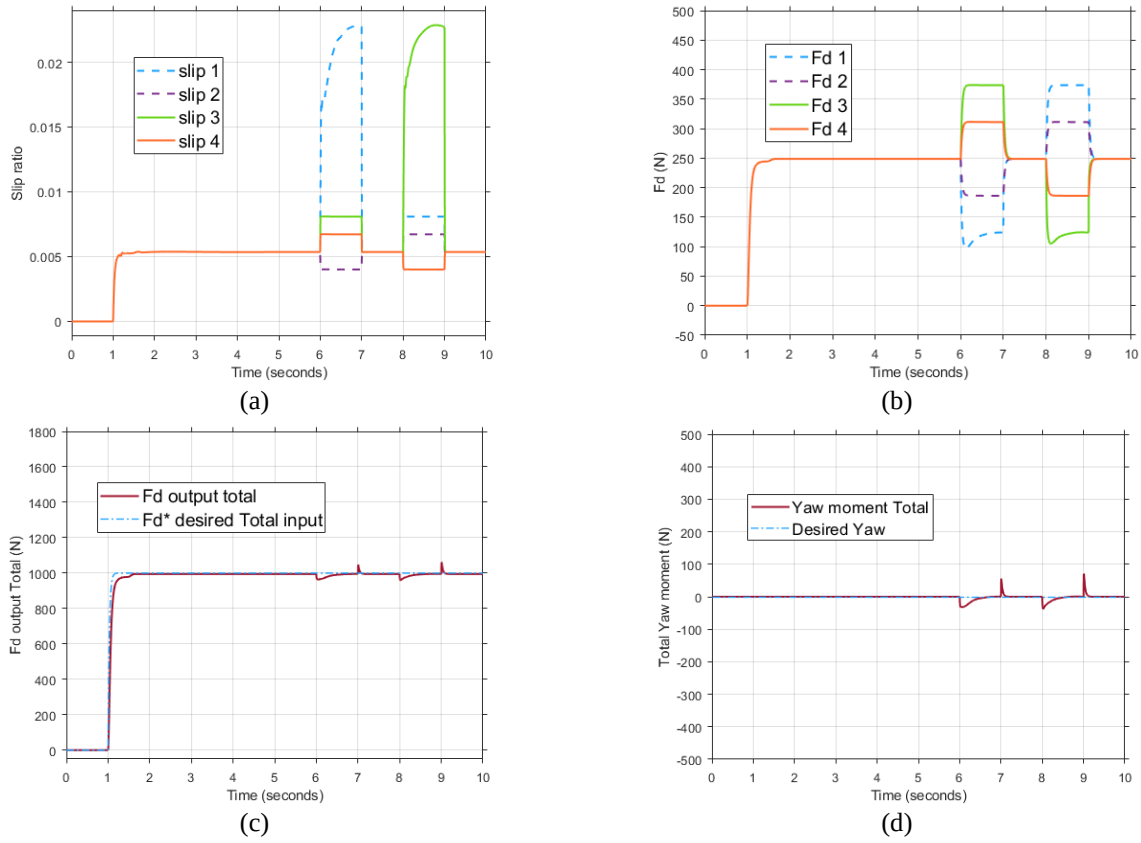

Figure 21. Simulation results of split slippery sheet (PD-Fuzzy control and distribution method). (a) Slip ratio, (b) driving force F_d (c) total output driving force $F_{d\ total}$ (d) Yaw-moment output.

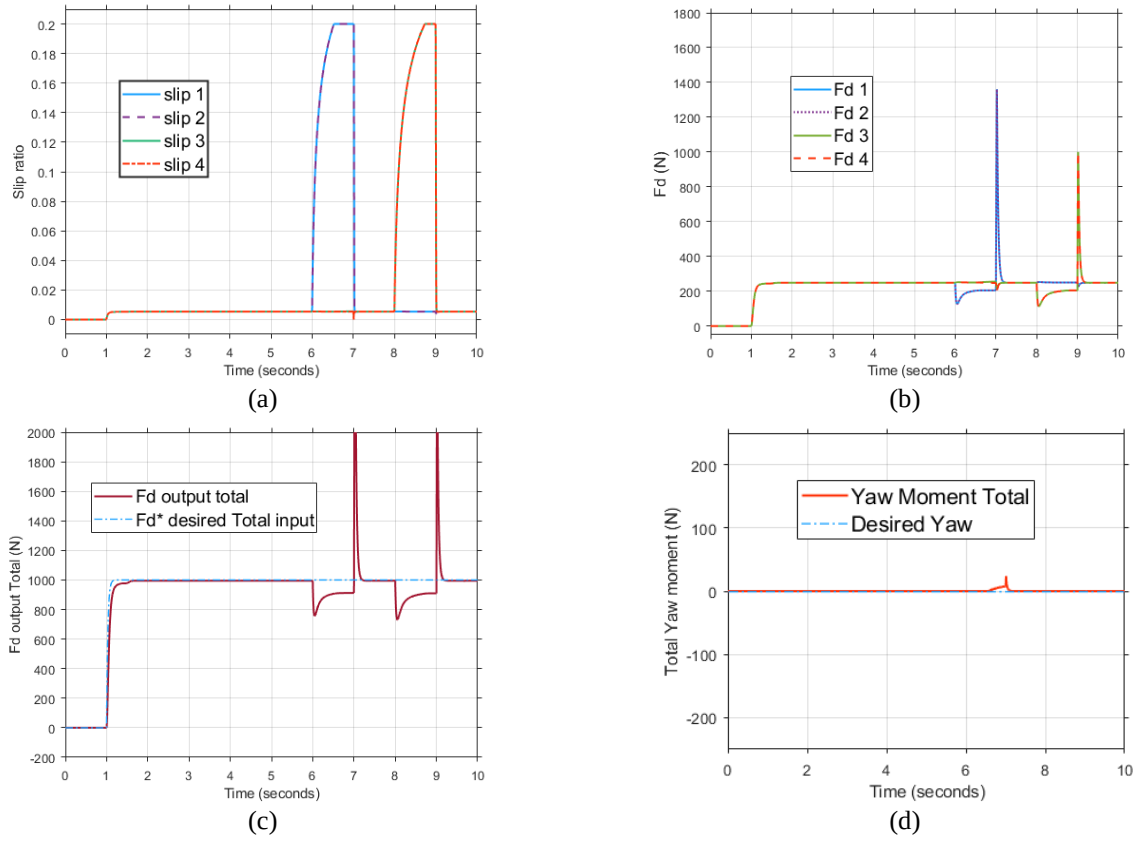

Figure 22. Simulation results of full slippery sheet (only PD-Fuzzy control). (a) Slip ratio, (b) driving force F_d (c) total output driving force $F_{d\ total}$ (d) Yaw-moment output.

The results of Slip ratio when the vehicle runs into a slippery sheet between 6-7th second for the front wheels and 8-9th second for the rear wheels is better than results without applying control, but it's still high and reached the upper limits for slip then saturated. In addition, there is a significant difference between vehicle speed and wheels speed. As a result, the driving forces and delivered torque for each wheel are reduced and saturated when slip occurs. Consequently, the total output driving force did not retain which means the slippery sheet effects significantly on the traction operation and vehicle stability.

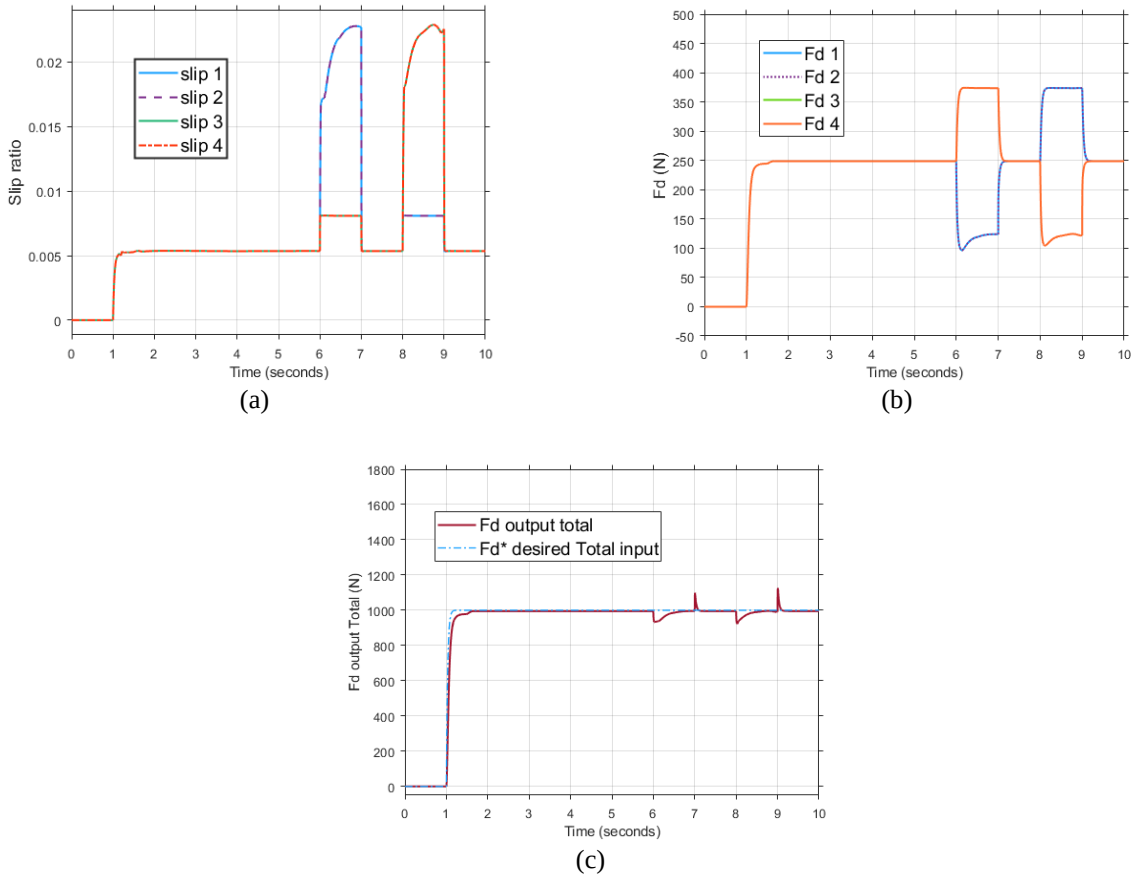

Figure 23. Simulation results of full slippery sheet (PD-Fuzzy control and distribution method). (a) Slip ratio, (b) driving force F_d (c) total output driving force $F_{d\ total}$

Figures 23 describes simulation results of the proposed control system with the proposed distribution method when vehicle move on the second experimental road. The Total input driving force distributed between the front and rear wheels based on which wheel still have traction on normal road. Consequently, the delivered torques for each wheel are distributed too.

As a result, the slip ratio results while applying distribution strategies when the vehicle moves on a split slippery sheet are too small and didn't exceed (0.025) for all wheels when its moves on slippery surface. Which is a negligible slip for both of PD-Fuzzy and PI controller. The same results proofed by comparing the vehicle speed and wheels speed for both of the two controllers. The total driving force for both of PD-Fuzzy and PI are retained without effects on the traction operation, prevent slip ratio from reach to saturation levels, also the Yaw-moment equal to zero, which can be confirmed by comparing figures (22) with (23).

The results of the total output driving force and total output yaw-moment for both of PD-Fuzzy and PI controller while the vehicle moves on split and full slippery sheet are compared, as shown in Figures 24 and 25.

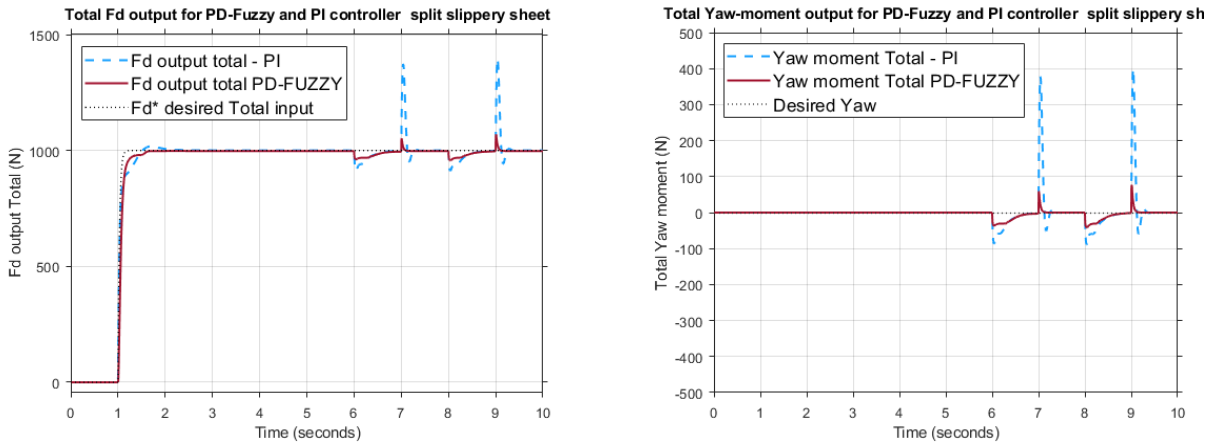

(a) (b)

Figure 24. Simulation results of split slippery sheet (PD-Fuzzy logic and PI-control with distribution). (a) Total output driving force $F_{d\ total}$ (b) Yaw-moment output.

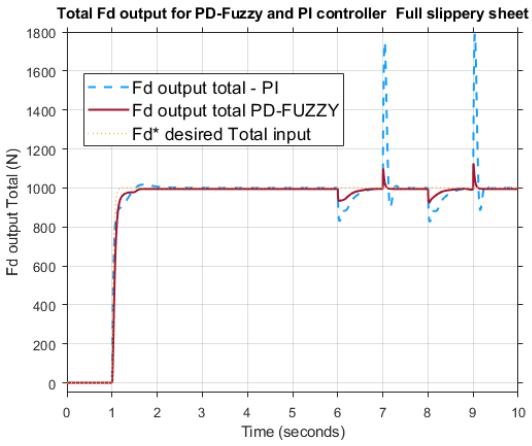

Figure 25. Simulation results of full slippery sheet (PD-Fuzzy logic and PI-control with distribution). Total output driving force $F_{d\ total}$

Both of PD-Fuzzy controller and PI controller reduced slip, retained total driving force, suppressed yaw-moment, and improve the stability of the electric vehicle. However, the performance of the proposed driving force control based on PD-Fuzzy controller as wheel speed controller is better than that of the PI controller for the same simulation condition.

PI controller retained the total requested driving force but with a significant instability after moving on the short split/full slippery sheet. Also the total generated yaw moment is much larger than the one based on PD-Fuzzy controller, which reduce the vehicle performance and effects on the traction operation while the vehicle moves on the split or slippery sheet.

In the contrast, the proposed control system based on PD-Fuzzy as a wheels speed controller proof that it can keep the total driving force and yaw-moment too close to the optimal required values. The system response based on the PD-Fuzzy controller is smoother, faster, and has negligible error while the vehicle moves on the split or slippery sheet.

5. Conclusions

Four-wheel driving force distribution method for instantaneous split/full slippery surface road is proposed. However, the response of the proposed driving force control based on PD-Fuzzy

controller as a wheel speed controller is better than that of the PI controllers for the same simulation conditions. The simulation outcomes demonstrate that by applying the proposed force distribution control system the generation of yaw-moment and reduction of the total driving force is prevented. Also slip and traction operation controlled with high performance, which means stable driving despite road conditions is achieved.

In future, in order to increase the reliability of the control system, implementing vehicle dynamics with taking into account the lateral and longitudinal motion of the vehicle, and depending on the online real-time estimation of longitudinal and lateral slip values to find the optimal solution for optimization function are suggested.

Authors' Contributions

Islam Shamia and Kemal Keskin designed the structure. Problem definition has been made by Kemal Keskin according to the studies in the literature, while mathematical model has been clarified by Islam Shamia. The setting of test environment and experimental work were done by Islam Shamia and Kemal Keskin, and both authors wrote up the article. Both authors read and approved the final manuscript.

Competing Interests

The authors declare that they have no competing interests.

References

[1]. Jalali K., Uchida T., McPhee J., Lambert S., Development of a Fuzzy Slip Control System for Electric Vehicles with In-wheel Motors, SAE International Journal of Alternative Powertrains. SAE International, 2012, 1: 46–64.

[2]. Fazelpour F., Vafaeipour M., Rahbari O., Rosen MA., Intelligent optimization to integrate a plug-in hybrid electric vehicle smart parking lot with renewable energy resources and enhance grid characteristics. Energy Conversion and Management, 2014, 77: 250–61.

[3]. Xu W., Chen H., Zhao H., Ren B., Torque optimization control for electric vehicles with four in-wheel motors equipped with regenerative braking system, Mechatronics, 2019, 57: 95–108.

[4]. Wong A., Kasinathan D., Khajepour A., Chen S-K., Litkouhi B., Integrated torque vectoring and power management framework for electric vehicles, Control Engineering Practice, 2016, 48: 22–36.

[5]. Wang Z., Qu C., Zhang L., Xue X., Wu J., Optimal Component Sizing of a Four-Wheel Independently-Actuated Electric Vehicle With a Real-Time Torque Distribution Strategy, IEEE Access, 2018, 6: 49523–49536.

[6]. Chiang W-P., Yin D., Shimizu H., Slip-based regenerative ABS control for in-wheel-motor drive EV, Journal of the Chinese Institute of Engineers, 2014, 38(2): 220–31.

[7]. Maeda K., Fujimoto H., Hori Y., Four-wheel Driving-force Distribution Method for Instantaneous or Split Slippery Roads for Electric Vehicle, Automatika, 2013, 54(1): 103–113.

[8]. Fujimoto H., Harada S., Model-Based Range Extension Control System for Electric Vehicles With Front and Rear Driving–Braking Force Distributions, IEEE Transactions on Industrial Electronics, 2015, 62(5): 3245–3254.

[9]. Hori Y., Toyoda Y., Tsuruoka Y., Traction control of electric vehicle: basic experimental results using the test EV "UOT electric march", IEEE Transactions on Industry Applications, 1998, 34(5), 1131–1138.

[10]. Peng H., Hori Y., Optimum traction force distribution for stability improvement of 4WD EV in critical driving condition, 9th IEEE International Workshop on Advanced Motion Control, 2006.
[11]. Yuan L., Zhao H., Chen H., Ren B., Nonlinear MPC-based slip control for electric vehicles with vehicle safety constraints, Mechatronics, 2016, 38, 1–15.
[12]. Yinghui G., Chang C., Torque distribution control for electric vehicle based on traction force observer, 2011 IEEE International Conference on Computer Science and Automation Engineering 2011.
[13]. Dejun Y., Hori Y., A new approach to traction control of EV based on maximum effective torque estimation, 2008 34th Annual Conference of IEEE Industrial Electronics, 2008.
[14]. Guangcai, Z., Yugong, L., Keqiang, L., Xiaomin, L., Slip ratio control of independent AWD EV based on fuzzy DSMC, 2007 IEEE International Conference on Vehicular Electronics and Safety 2007.
[15]. Jin L-Q., Ling M., Yue W., Tire-road friction estimation and traction control strategy for motorized electric vehicle, Hu X, editor. PLOS ONE. Public Library of Science (PLoS), 2017, 12(6), e0179526.
[16]. Dizqah AM., Lenzo B., Sorniotti A., Gruber P., Fallah S., De Smet J,. A Fast and Parametric Torque Distribution Strategy for Four-Wheel-Drive Energy-Efficient Electric Vehicles, IEEE Transactions on Industrial Electronics, 2016, 63(7), 4367–76.
[17]. Li Y., Li B., Xu X., Sun X., A Nonlinear Decoupling Control Approach Using RBFNNI-Based Robust Pole Placement for a Permanent Magnet In-Wheel Motor, IEEE Access, 2018, 6, 1844–1854.
[18]. Li Y., Deng H., Xu X., Jiang H., Review on torque distribution strategies for four in-wheel motor drive electric vehicles, IOP Conference Series: Materials Science and Engineering, 2018, 042041.
[19]. Zhao B., Xu N., Chen H., Guo K., Huang Y., Design and Experimental Evaluations on Energy-Efficient Control for 4WIMD-EVs Considering Tire Slip Energy, IEEE Transactions on Vehicular Technology, 2020, 69, 14631–44.
[20]. Moore, D. F., The friction of pneumatic tyres, Elsevier Scientific Publishing Company, 1975.
[21]. Gillespie, T. D., Fundamentals of vehicle dynamics, Society of automotive engineers Warrendale, SAE International, 1992.
[22]. Siampis, E., Optimal torque vectoring control strategies for stabilisation of electric vehicles at the limits of handling, PhD dissertation, Cranfield University, 2016.
[23]. Jazar, R. N., Vehicle dynamics: theory and application, Springer, 2017.
[24]. Pacejka HB, Bakker E. The Magic Formula Tyre Mode, Vehicle System Dynamics, 1992, 27, 1–18.
[25]. McTrustry, S. C., Modelling and control of electric vehicles with individually actuated in-wheel motors, Master Thesis, University of Wollongong, 2016.